Multidimensional Thermal-Hydraulic Analysis for Decay Heat Exchanger of PGSFR

Jonggan Hong*, Jung Yoon, Dehee Kim, Tae-Ho Lee
Korea Atomic Energy Research Institute, 989-111 Daedeok-daero, Yuseong-gu, Daejeon, 305-353, Korea
**Corresponding author: hong@kaeri.re.kr*

1. Introduction

The decay heat exchanger (DHX) of PGSFR is a shell-and-tube type counter-current flow sodium-sodium heat exchanger, and each unit is designed for the rated thermal power of 1.0 MWt, which is corresponding to the nominal design capacity of a single passive decay heat removal system (PDHRS) and active decay heat removal system (ADHRS) loops. The DHX unit is fully immersed in the cold sodium pool region and removes the system heat load sufficiently and reliably during the temperature transient [1, 2].

In this work, a multidimensional thermal-hydraulic analysis for the DHX was carried out numerically and the numerical results were compared with the calculated results of the 1-D DHX design code to verify the reliability of the design code [3]. In addition, an influence of the cold pool sodium which flows into the shell-side of the DHX through the shell outlet was evaluated.

2. Numerical Method

Numerical simulations were carried out using the commercial computational fluid dynamics package, STAR-CCM+ V9.02.007. The axisymmetric steady-state governing equations for continuity, momentum and energy were solved with 1/4 DHX domains (Fig. 1), and the conjugate heat transfer methodology was applied for the thermal interaction between the solid and fluid. The standard k-ε model (cubic) and two-layer all y+ wall treatment were employed as the turbulent model. Radiation through Ar region was calculated with the S2S model. Properties of the sodium, 9Cr-1Mo-V steel, and Ar were given as a function of the temperature.

Basically, a computational geometry follows the geometry of the PGSFR DHX [2]. In this work, two different DHX domains were prepared to evaluate an influence of a buffer region at the shell outlet. One DHX domain (Fig. 1a) has the sodium buffer region between the shell outlet and lower tubesheet, and the other (Fig. 1b) has no sodium buffer region. Each DHX domain consists of the shell-side sodium, tube-side sodium, Ar gas, and 9Cr-1Mo-V structure. A cold pool domain (Fig 1d) was also made to simulate the cold pool sodium coming into the shell outlet.

A polyhedral mesh with prism layer cells was generated on the geometric domains. The base size in the region except the cold pool was 5.0 mm and that of the cold pool was 10 mm. Fig. 2 shows vertical and horizontal cross sections of the generated mesh which has 29,192,512 cells.

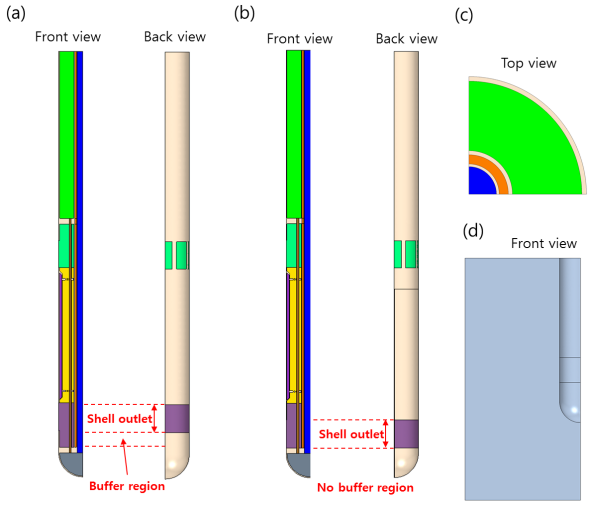

Fig. 1 3-D axisymmetric computational domains; (a) 1/4 DHX domain #1, (b) 1/4 DHX domain #2, (c) Top view of the DHX domain, and (d) cold pool.

Three cases were analyzed by the numerical simulation as Table I. The DHX of the case 1 and 2 had a buffer region like Fig 1a, but that of the case 3 did not have a buffer region like Fig 1b. All the values of the temperature and flow rate in boundary conditions were chosen based on the design point of the PGSFR DHX [2]. In the case 1, a mass flow inlet condition was applied at the outlets of both the shell- and tube sides along with a negative number of the mass flow rate to eliminate an inflow of the cold pool sodium and the cold pool domain (Fig. 1d) was not included. In the case 2 and 3, the mass flow inlet condition at the inlets and pressure outlet condition at the outlets were applied and the cold pool domain was added so as to simulate the inflow of the cold pool sodium.

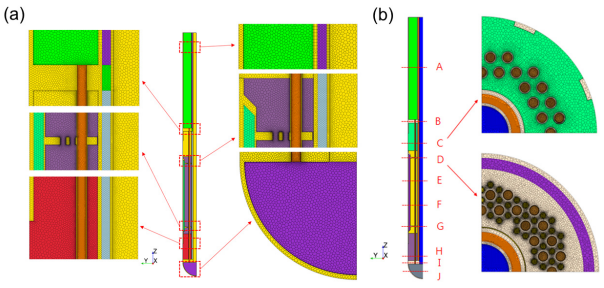

Fig. 2 Computational mesh generation; (a) vertical cross section and (b) horizontal cross section.

Table I: Buffer region and boundary conditions for each case.

Case	Buffer region	Boundary conditions
1	Y (Fig. 1a)	1) Tube inlet (pressure outlet) Pressure: 0.0 Pa, Temp: 195.7℃ 2) Tube outlet (mass flow inlet) Flow rate: –1.095 kg/s, Temp: 370℃ 3) Shell inlet (pressure outlet) Pressure: 0.0 Pa, Temp: 390℃ 4) Shell outlet (mass flow inlet) Flow rate: –1.25 kg/s, Temp: 390℃ 5) Outer surface of shroud: Adiabatic
2	Y (Fig. 1a)	1) Tube inlet (mass flow inlet) Flow rate: 1.095 kg/s, Temp: 195.7℃ 2) Tube outlet (pressure outlet) Pressure: 0.0 Pa, Temp: 370℃ 3) Shell inlet (mass flow inlet) Flow rate : 1.25 kg/s, Temp: 390℃ 4) Shell outlet (pressure outlet) Pressure: 0.0 Pa, Temp: 390℃ 5) Outer surface of shroud: Adiabatic
3	N (Fig. 1b)	The same as Case 2

Table II: Numerical results vs. SHXSA calculation results.

		Case 1	Case 2	Case 3	SHXSA
Shell	Outlet temp., ℃	238.1	369.6	368.1	236.4
	Power, MW	0.249	-	-	0.250
	Pressure drop, Pa	136	139	138	210
Tube	Outlet temp., ℃	376.1	373.8	374.1	370.0
	Power, MW	0.261	0.258	0.258	0.250
	Pressure drop, Pa	678	678	673	417

3. Numerical Results

Table II shows the comparison between the numerical results and SHXSA calculation results. The inflow of the cold pool sodium was suppressed by the boundary condition in the case 1 (Fig. 3), and the outlet temperatures and the power of the numerical results were in good agreement with those of the SHXSA results. In the case 1, the deviations in the outlet temperatures and the power were 0.72-1.65% and –0.4-4.4%, respectively. However, in the case 2 and 3, the inflow of the cold pool sodium was obviously observed (Fig. 3). Thus the outlet temperature of the shell-side in the case 2 and 3 was much higher than that in the case 1. The power of the shell-side could not be compared with the SHXSA result because the SHXSA code does not consider the inflow of the cold pool sodium. The outlet temperature and power in the tube-side of the case 2 and 3 were similar to those of the case 1. Thus it was found that the inflow of the cold pool sodium and the existence of the buffer region rarely affected the overall heat transfer performance of the DHX.

When the inflow of the cold pool sodium occurred at the shell outlet and the DHX did not have the buffer region (case 3; Fig. 4b), the radial sodium temperature variation at the lower part (section H) of the shell-side increased considerably. It caused a large radial variation in the temperature of the lower tubesheet below, which would be harmful in terms of the thermal stress.

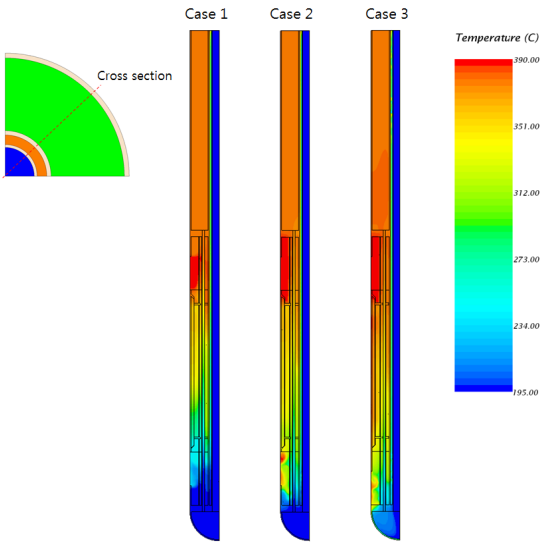

Fig. 3 Temperature distribution in the vertical cross section.

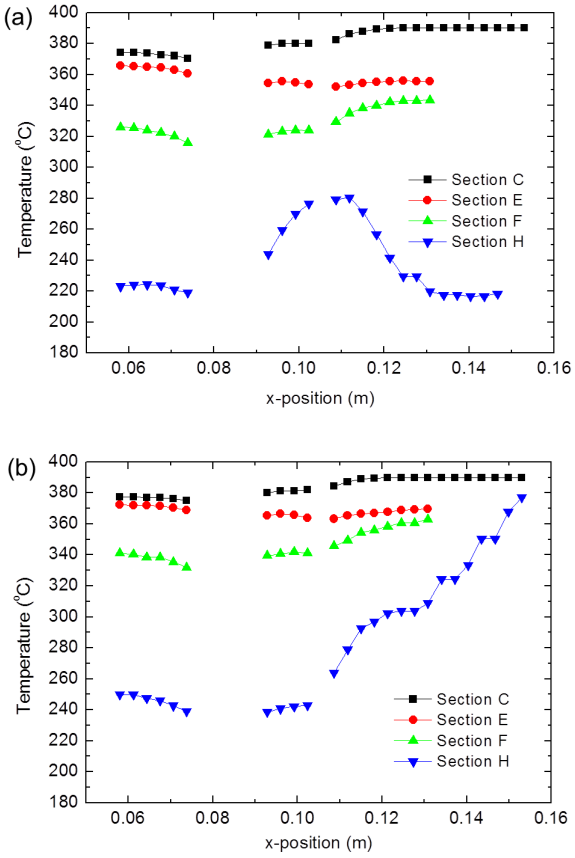

Fig. 4 Radial sodium temperature variation of the shell-side in the horizontal cross sections C, E, F, and H; (a) case 2 and (b) case 3.

The pressure drop was also rarely affected by the inflow of the cold pool sodium and the existence of the buffer region (Table II). The SHXSA was found to be conservative in predicting the pressure drop of the

shell-side by about 35% because it did not consider the small gap (2 mm) between the grid plate and inner cylinder. However, in the case of the tube-side, the pressure drop by the SHXSA code was about 60% smaller than that by the numerical simulation. In the numerical method, a pressure drop by the vortex in the lower sodium chamber was calculated unlike the SHXSA code, and the pipe connected to the tubes was almost twice the length of the one in the SHXSA code.

4. Conclusions

Multidimensional thermal-hydraulic analysis for the DHX of PGSFR was conducted numerically. The numerically-obtained outlet temperatures and power of the DHX showed good agreement with the SHXSA results. The SHXSA code was conservative in calculating the pressure drop of the shell-side which is our major concern in designing the natural circulation of the decay heat removal system. It was revealed that the buffer region is needed to reduce the thermal stress in the lower tubesheet by the inflow of the cold pool sodium.

ACKNOWLEDGMENTS

This work was supported by the National Research Foundation of Korea (NRF) grant funded by the Korea government (MSIP). (No. 2012M2A8A2025624).

REFERENCES

[1] J. H. Eoh, Conceptual Design Report of PGSFR DHX, KAERI Internal Document, SFR-514-DF-462-001, 2012
[2] J. Hong, DHX Sizing Calculation, KAERI Internal Document, SFR-514-DF-302-002, 2014
[3] J. Hong, Report on Multi-dimensional Thermal-Hydraulic Analysis of DHX, SFR-514-DF-302-003, 2015